

# Synthesis of poly(aniline-co-*o*-toluidine) nanocolloidal particles in aqueous poly(styrene sulfonic acid) by dispersion polymerization method

D. Manoharan · J. Chandrasekaran ·  
S. Maruthamuthu · P. Kathirvel · P. Jayamurugan

Received: 18 September 2014 / Accepted: 1 December 2014 / Published online: 11 December 2014  
© The Author(s) 2014. This article is published with open access at Springerlink.com

**Abstract** Nanocolloidal poly(aniline-co-*o*-toluidine) particles were synthesized by dispersion polymerization using different weight ratios of steric stabilizer poly(styrene sulfonic acid). The dispersed nanocolloidal particles ranging from 10 to 100 nm were inspected by transmission electron microscopy and particle size analyzer. The strong doping level of particles at higher weight ratios of stabilizer was analyzed by elemental analysis. The functional groups of particles were identified by Fourier transform-infrared spectra. A reduction of the conjugation length in the particles leads to the homogeneous mixture of phases which was confirmed by scanning electron microscopy and UV–visible spectra. The blue shift polaron band has confirmed the change in conjugation length of the particle. High thermal stability of particles was examined by thermogravimetry analysis.

**Keywords** Nanomaterials · Polymer synthesis · Colloids · Thermal properties · Transmission electron microscopy

## Introduction

Recent development in organic electronics has brought a colossal momentum in the field of electrically conductive and semiconductive polymers. The conducting polymers are employed as functionalized materials and play a vital role in diversified applications [1]. Among the promising conducting polymers, polyaniline (PANI) has received great attention from researchers in the last decade because of easy synthesis, environmental stability, high conductivity, low cost, complex structure and special proton doping mechanism. The physical properties of conducting polymers have been controlled by oxidation and protonation elements as well [2–5]. The PANI has numerous applications that include organic lightweight batteries, microelectronic devices, electrochromic displays, electromagnetic shielding devices and sensors [6–12]. Since PANI exhibits poor physical and mechanical properties, researchers find very few applications and one of the challenges in PANI is the processability. It is insoluble in common organic solvents, which became the center point of several investigations. To overcome this disadvantage, several techniques have been followed such as substitution in the aniline monomer prior to polymerization, copolymerization with other monomers, making blends with other conventional polymers and preparation of dispersed colloidal polymers [13–17]. The colloidal PANI particles are produced by oxidation of aniline in the presence of suitable water-soluble polymer [18, 19]. In the process of dispersion polymerization, the monomer is soluble in the reaction

---

D. Manoharan · J. Chandrasekaran (✉)  
Department of Physics, Sri Ramakrishna Mission Vidyalyaya  
college of Arts and Science, Coimbatore 641020, Tamil Nadu,  
India  
e-mail: jchandaravind@yahoo.com

S. Maruthamuthu  
Research and Development Centre, Bharathiar University,  
Coimbatore 641046, Tamil Nadu, India

S. Maruthamuthu  
Department of Physics, Dr. Mahalingam College of Engineering  
and Technology, Pollachi 642003, Tamil Nadu, India

P. Kathirvel  
Department of Sciences, School of Engineering, Amrita Vishwa  
Vidyapeetham, Coimbatore 641112, Tamil Nadu, India

P. Jayamurugan  
Department of Physics, Adhiyamaan College of Engineering,  
Hosur 635109, Tamil Nadu, India

medium, but the resultant polymer is insoluble under the same condition and the polymer precipitation is prevented by the presence of water-soluble polymer, the so-called steric stabilizer [20]. The colloidal PANI particles have a typical average particle size around hundred nanometers and thus are denoted as nanocolloids. The nanometer-sized PANI particles have been used for practical applications such as antistatic coatings, supercapacitors, corrosion production, chemical sensors, batteries and nanodevices [21–24]. Although there is a lack of facilities and reliable techniques for preparing high-quality nanometer-sized particles, researchers have employed different methods using chemical or electrochemical, electrospinning interfacial and microwave polymerization [19, 25–28]. The polymer synthesis using aniline derivative *o*-toluidine has also attracted considerable attention since they exhibit enhanced solubility and better processability than PANI [29, 30]. Hence synthesis of nano-sized copolymer of aniline with *o*-toluidine will have both the advantages of polytoluidine and PANI. Among the various water-soluble polymer poly(styrene sulfonic acid) (PSS) has been used as a dopant with polymer backbone to produce electrically conductive emeraldine salt forms. The excess of sulfonic acid group has enhanced the water dispersibility and resultant polymer is processable easily in application side [31, 32].

In the present work, nanocolloids of poly(aniline-co-*o*-toluidine) (PAT) are prepared easily with the presence of PSS through the dispersion polymerization method to get beneficial material with new synthetic properties. The different wt% of PSS with (aniline + *o*-toluidine) is used to understand the formation of dispersed nanocolloids in aqueous PSS. The spectroelectrochemical investigations of dispersed particles are discussed.

## Experimental method

### Materials

Two monomers aniline, *o*-toluidine and oxidant ammonium peroxydisulfate (APS) (Merck) were used to prepare copolymer. Polystyrene sulfonic acid (PSS) MW >75,000 (Aldrich) was used as a dopant and as a steric stabilizer. Deionized water was used for all the reactions.

### Polymerization of aniline and *o*-toluidine

The PAT:PSS colloidal particles were synthesized using dispersion polymerization. In this typical synthesis, different wt% of PSS was dissolved in 90 ml of deionized water in a reaction vessel and the two monomers, 0.4657 g (5 mmol) of aniline and 0.5359 g (5 mmol), of *o*-toluidine

were added slowly dropwise. Aniline and *o*-toluidine were dissolved thoroughly in the aqueous solution of the steric stabilizer; PSS with the aid of ultrasonication. The different wt% of PSS was maintained as 0.5, 1, 2.5, 5, 10 and 15. An amount of 2.28 g (10 mmol) of ammonium peroxydisulfate was dissolved in 10 ml of deionized water with the help of ultrasonication and then slowly added into the solution of monomers with polymeric acid PSS. The polymerization was carried out for 24 h at 5 °C with constant mechanical stirring. The presence of the stabilizer with different wt% affected the course of polymerization. The stable colloidal dispersions were obtained by sufficiently high (i.e., >1 wt%) stabilizer concentration. The low (i.e., ≤1 wt%) concentration of stabilizer yielded precipitation in the reaction vessel. The stable colloidal dispersions have been precipitated with excess of ethanol to obtain the solid form of PAT:PSS particles. The precipitated powders were dried at 60 °C in vacuum for 24 h.

### Nanocolloidal particle formation

The oxidation of aniline and its derivative *o*-toluidine with ammonium peroxydisulfate is exothermic. The hydrogen atoms of aniline and *o*-toluidine are released in the form of protons. The decomposition of peroxydisulfate produced the sulfuric acid in the reaction medium. When the polymerization is carried out in the absence of any acid (i.e., without dopant), the monomers aniline and *o*-toluidine are protonated by the sulfuric acid in the reaction medium. Simultaneously, the protonated aniline cations are being involved in the polymer chain formation. The final product of aniline and *o*-toluidine oxidation in water without initial dopant is thus composed of both oligomeric and polymeric components [32]. The initial proton to monomer affects the polymer morphology. The acidity of the reaction medium affects the proportion between the neutral aniline molecules and anilinium cations. Generally the oxidation of protonated anilinium cation is difficult compared to the oxidation of neutral aniline. In this present work PSS is used as initial protonator and as well as steric stabilizer. The initial proton concentration is controlled by changing the wt% of PSS in the reaction medium. When the PSS wt% is less than the monomers, the reaction medium is occupied by more number of neutral aniline molecules and less number of anilinium cations. The poly(aniline-co-*o*-toluidine) precipitation is yielded in the reaction vessel by the oxidation of aniline and *o*-toluidine with less or equal wt% of PSS. When the PSS wt% is higher than the monomers weight, the reaction medium is fully occupied by anilinium cations and an excess of PSS. The oxidation of anilinium cations yielded poly(aniline-co-*o*-toluidine):poly(styrene sulfonic acid) nanocolloidal particles and the excess of PSS can serve as the stabilizer. For lower

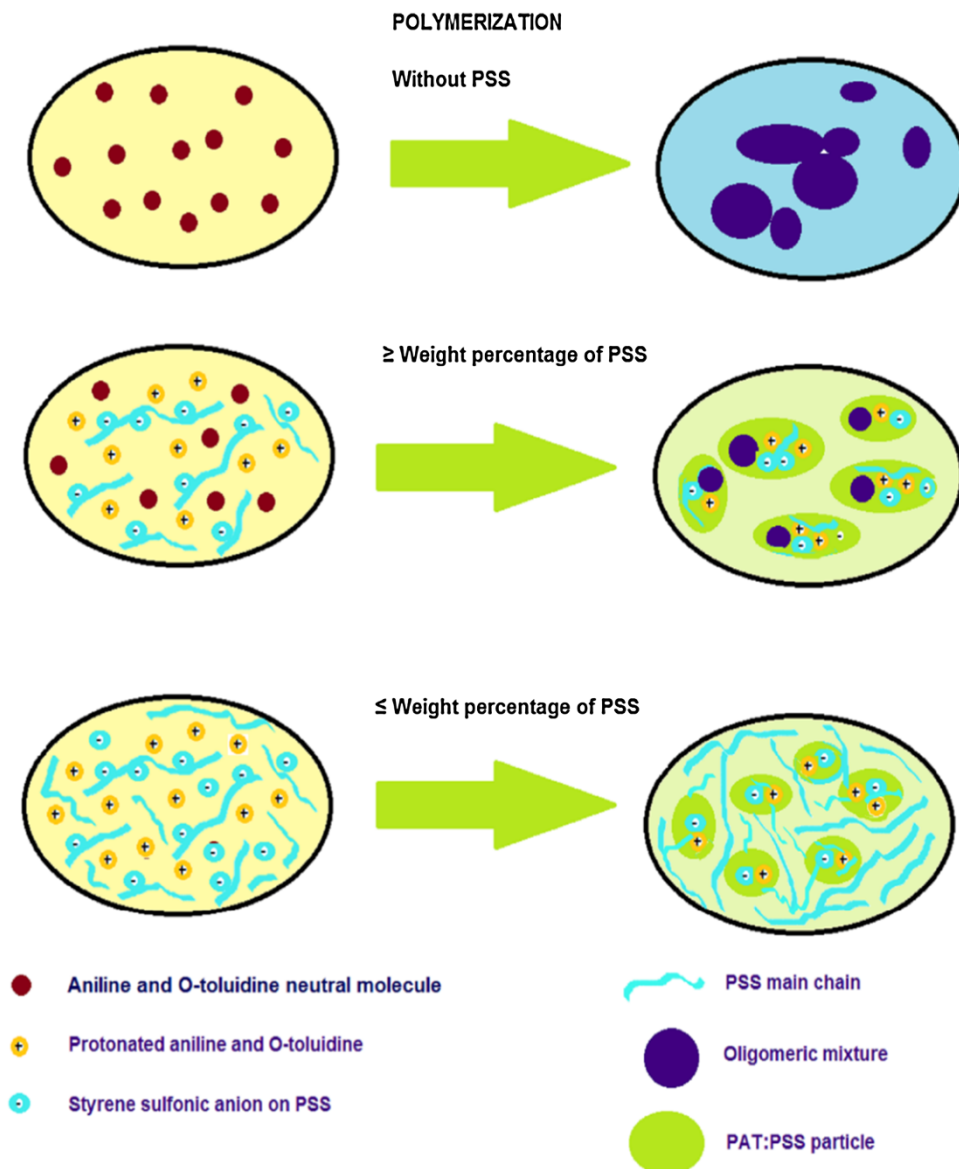
PSS content the PAT particles are formed in larger size by aggregation of large number of particles. Increase facilitates regular shape and alignment of the nanoparticles. The interaction between the nanoparticles is hindered by the excess number of PSS molecules. Hence, higher wt% of PSS stabilized the dispersions and decreased the PAT particle size. The nanocolloidal formation is depicted in Scheme 1.

#### Characterization techniques

The water-dispersible PAT:PSS nanoparticles were precipitated with excess of ethanol to obtain the solid form of PAT:PSS nanoparticles. The higher wt% of PSS required more quantity of ethanol. Thus, undoped PAT particles

were extracted without ethanol. The FT-IR spectra of various samples in KBr pellets were obtained using a Bruker IFS 66 V IR spectrophotometer. The detailed PAT compositions with different PSS wt% were performed by elemental analysis using Elementar Vario EL III. Perkin-Elmer Lambda 35 UV–Vis spectrometer was used for UV–Vis spectral analysis. The particles were dispersed in DI water for UV–Vis measurements using DI water as the blank. Morphological studies of PAT:PSS powders were performed by SEM technique with JEOL scanning electron microscope (Model JSM-6390). The particle size and size distribution of various samples were determined by laser light scattering with a Zetasizer particle size analyzer (Malvern, UK). Each suspension was diluted to the appropriate concentration with double-distilled water

**Scheme 1** Colloidal formation of PAT:PSS particles



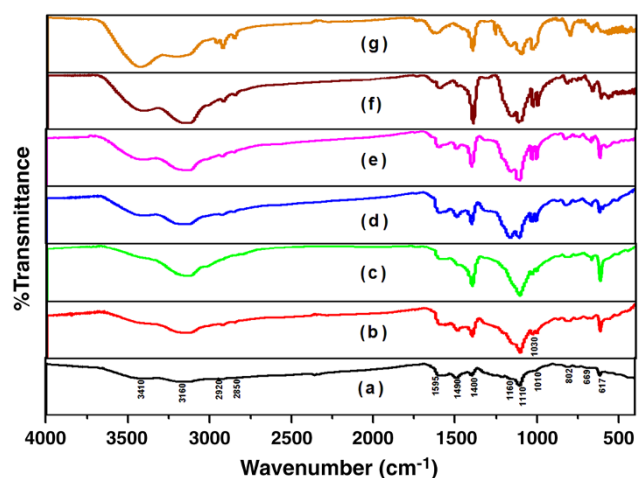


**Fig. 1** FT-IR spectra of PAT particles **a** synthesized without PSS and synthesized with different weight ratios of PSS **b** 0.5, **c** 1, **d** 2.5, **e** 5, **f** 10 and **g** 15

before the measurements. Transmission electron microscopy observation was performed using an EOL-1200 EX transmission emission microscope operated at a 100 kV accelerating voltage. Specimens for TEM were prepared by spreading a small drop of the sample solution onto a 400 mesh copper grid. Thermal analysis of various samples was conducted using a DuPont TA Instrument 2050 thermo gravimetric analyzer under a dry nitrogen atmosphere, with a heating rate of 20 °C/min and using platinum pans. The temperature range was from 100 to 800 °C.

## Result and discussion

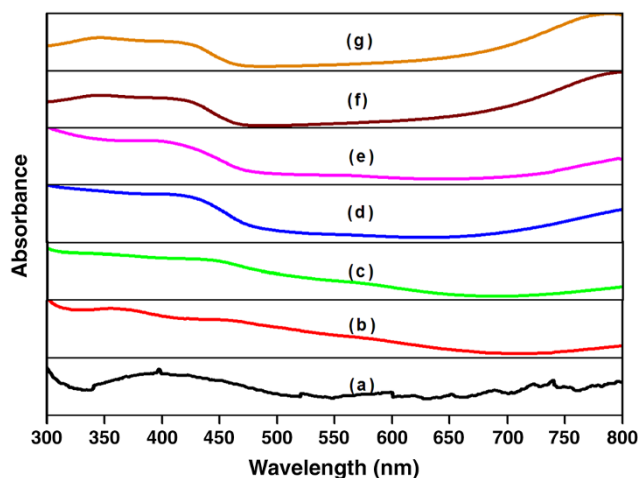
### FT-IR spectra

Figure 1 shows the FT-IR spectra of the PAT:PSS particles in the undoped and PSS-doped form. The PAT particles synthesized without protonator show the peaks at 617, 802, 1,010, 1,160, 1,400, 1,490, 1,595, 2,850, 2,920, 3,160 and 3,410  $\text{cm}^{-1}$ . The PAT particles polymerized with different wt% of PSS show the new peak at 1,030  $\text{cm}^{-1}$ . The FT-IR spectra ranging from 2,500 to 4,000  $\text{cm}^{-1}$  reflect particularly hydrogen bonding. The peak around 3,410  $\text{cm}^{-1}$  is assigned to  $-\text{NH}-$  stretching vibration of secondary amine groups. The increase in intensity of the peak at 3,410  $\text{cm}^{-1}$  is connected to water absorption; the PSS increases the hydrophilicity of the polymer particles. The peak at 3,160  $\text{cm}^{-1}$  is attributed to  $-\text{NH}-$  groups with strong H bonds formed between  $-\text{NH}-$  and  $-\text{N}=\text{}$  groups in the polymer chain. The small peaks at 2,920 and 2,850  $\text{cm}^{-1}$  are assigned to C–H asymmetric and symmetric stretching vibration mode of methyl groups. The gradual increase in intensity of the peaks with PSS wt% indicates that more *o*-

**Table 1** Elemental analysis of PAT particles synthesized without and with different weight ratios of PSS

Weight ratios of PSS	C %	H %	N %	S %	S/N
0	50.91	5.59	10.27	8.14	0.3463
0.5	49.82	7.9	9.25	9.31	0.4397
1	38.12	10.24	11.93	12.8	0.4688
2.5	46.58	8.92	7.95	9.95	0.5468
5	44.07	7.85	7.26	10.75	0.6469
10	44.01	10.67	6.25	11.16	0.7801
15	43.17	10.29	5.7	11.74	0.8998

toluidine segments are participated in the polymer chain. The peaks 1,595 and 1,490  $\text{cm}^{-1}$  are attributed to quinoid imine and benzenoid amine structure, respectively. The most intense peak at 1,400  $\text{cm}^{-1}$  is not straightforward. The above peak can be related to protonated nitrogen atoms of the polymer backbone or to ammonium sulfate by-product, deriving from APS and incorporated as “ionic cross linker” among PAT chains and/or among PAT and the polymeric stabilizer PSS chains [33]. The higher wt% of PSS shows the new peaks at 1,160 and 1,030  $\text{cm}^{-1}$ , which are attributed to asymmetric stretching and symmetric stretching vibration of sulfonic groups, respectively. The peaks at 1,110 and 617  $\text{cm}^{-1}$  are corresponding to S–C stretching vibration of PAT particles. The above peaks in PAT particles without PSS are associated to the presence of sulfuric acid, a by-product of APS. The asymmetric S–O stretching vibration is observed at the peak 669  $\text{cm}^{-1}$ . The para-coupled 1, 4-distributed out of plane C–H bonds are located in the region of 800–880  $\text{cm}^{-1}$ .



**Fig. 2** UV-visible spectra of PAT particles **a** synthesized without PSS and synthesized with different weight ratios of PSS **b** 0.5, **c** 1, **d** 2.5, **e** 5, **f** 10 and **g** 15

## Elemental analysis

Table 1 represents the composition of PAT particles synthesized with and without PSS. The PAT particle synthesized without PSS results in few sulfur groups, which is due to the by-product of sulfuric acid produced by the decomposition of APS. Hydrogen sulfate or sulfate counter ions always constitute a part of the PAT particles, when peroxydisulfate is used as an oxidant [32]. The S/N ratio of the particle represents the doping level of the polymer chain. The S/N ratio increases with PSS concentration which indicates the high doping level of PAT particles.

## UV–visible spectra

The optical absorption spectra of PAT particles with and without PSS are shown in the Fig. 2. The PAT particles synthesized without PSS show the absorption band at 405 nm due to the  $\pi$ - $\pi^*$  transition of the phenyl rings. The PAT particles doped with PSS show the three characteristic absorption bands at 330–360, 400–450 and around 800 nm. The absorption band at 330 nm exhibits due to the  $\pi$ - $\pi^*$

electron transition within benzenoid segment. The bands at 400–450 and 800 nm relate to the polaron band- $\pi^*$  transition and the  $\pi$ -localized polaron band transition in emeraldine salt, respectively. The polaron band intensity at 800 nm is gradually increased with PSS wt%, which is probably attributed to the doping level and/or to the higher electron density in the polymer backbone. Moreover, the blue shift is observed in the band at 800 nm with a higher wt% of PSS. The blue shift is attributed to increase in the number of side groups, which alter the torsional angle and leads to lower conjugation length of the particles.

## SEM

The SEM images of the synthesized PAT particles are shown in the Fig. 3. The PAT particles extracted using ethanol, are agglomerated into a complex structure and the actual morphology of single particle prediction becomes difficult. The phase separation between PAT and PSS is clearly noticed in Fig. 3a–e images with the formation of clusters and for Fig. 3f–g there are continuous particles with no smaller clusters. The higher wt% of PSS decreases

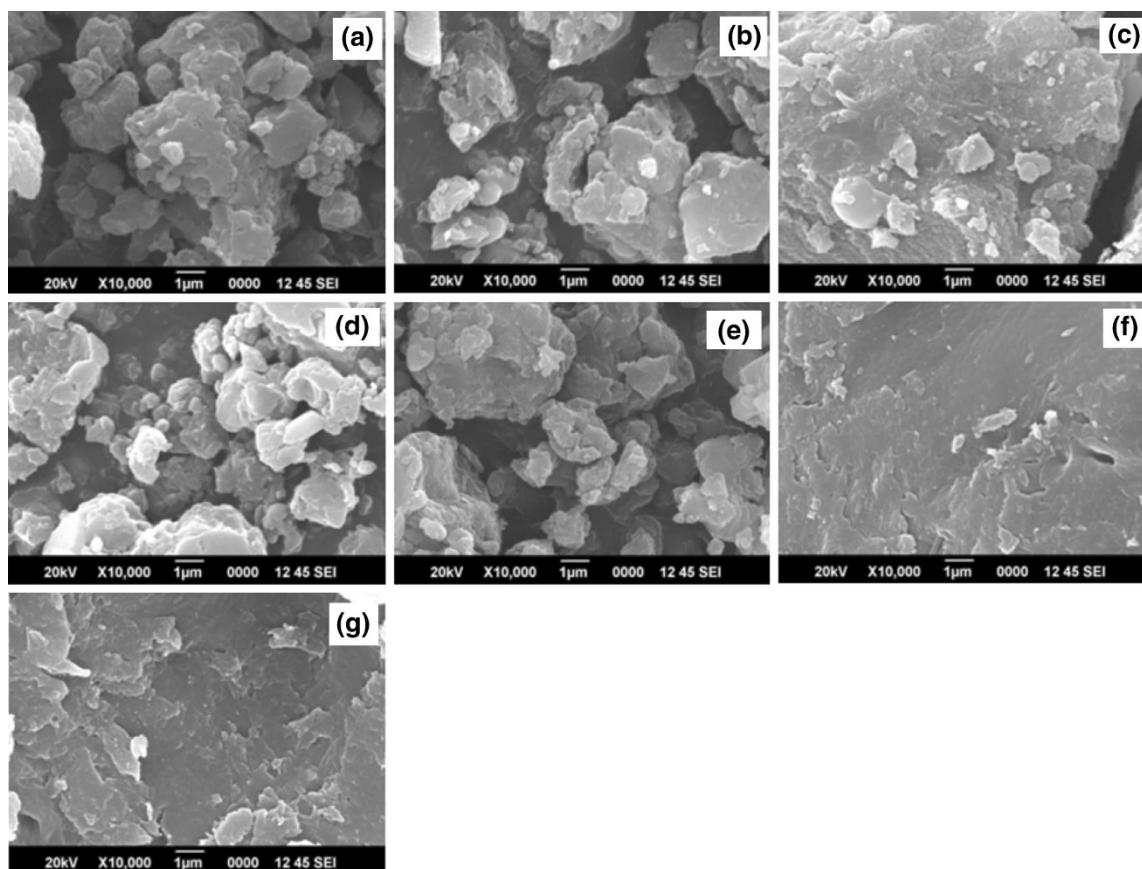


**Fig. 3** SEM images of PAT particles **a** synthesized without PSS and synthesized with different weight ratios of PSS **b** 0.5, **c** 1, **d** 2.5, **e** 5, **f** 10 and **g** 15

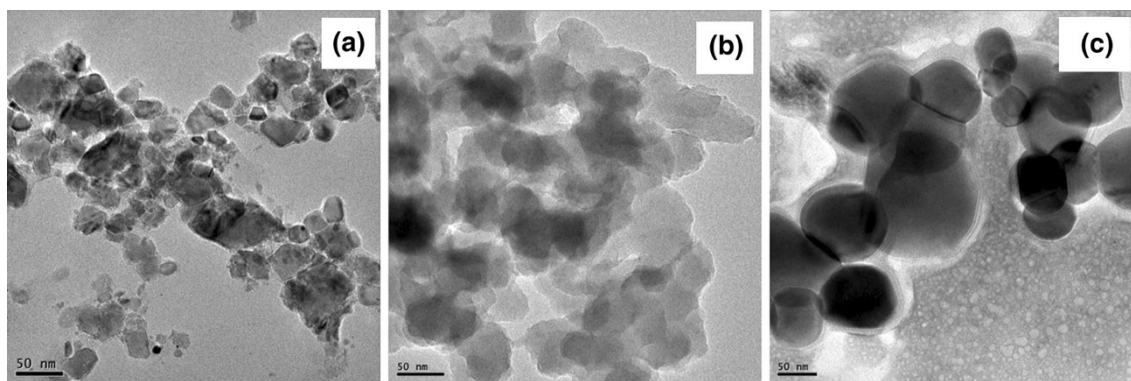


**Fig. 4** TEM images of PAT particles synthesized with different wt% of PSS **a** 0.5, **b** 1 and **c** 15

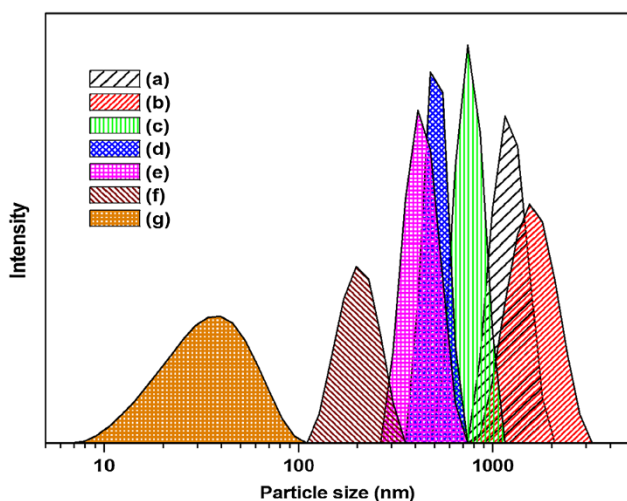


**Fig. 5** The particle size distribution profiles of PAT particles **a** synthesized without PSS and synthesized with different weight ratios of PSS **b** 0.5, **c** 1, **d** 2.5, **e** 5, **f** 10 and **g** 15

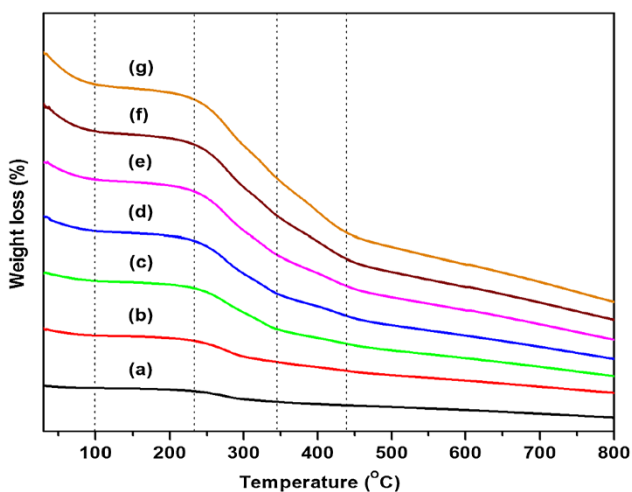


**Fig. 6** TGA curve of PAT particles **a** synthesized without PSS and synthesized with different weight ratios of PSS **b** 0.5, **c** 1, **d** 2.5, **e** 5, **f** 10 and **g** 15

the conjugation length of PAT particles, which enhances the particle size reduction with homogeneous mixture of phases and good compatibility.

#### TEM and particle size analyser

Closer inspection of TEM images of PAT:PSS particles are shown in the Fig. 4. The lower wt% of PSS 0.5 and 1 shows the network formation of the PAT particles. The higher wt% of PSS 15 resulted in the smooth and spherical particles with a size distribution of 40–100 nm. The network PAT particles for the lower wt% of PSS show the size distribution ranging from 500 nm to 2  $\mu$ m. The gradual increases of PSS stabilize the dispersions and decrease the PAT particle size. The particle size distribution profile of PAT particles with different wt% of PSS is shown in the Fig. 5. A wide distribution of particle size, 10–100 nm is observed for the higher wt% 15 of PSS. The nanocolloidal size distribution of PAT:PSS particles with 10–100 nm coincides with TEM image of higher wt% of PSS. The gradual decreases in the particle size from 2  $\mu$ m to around 100 nm reveals that the presence of stabilizer affects the course of polymerization. The stable nanocolloidal dispersions are exhibited only at sufficiently high stabilizer concentration.

#### TGA

The thermal stability of PAT particles in the presence of different wt% of PSS is studied by TGA. Figure 6 shows the curves of weight loss versus temperature for PAT:PSS particles. Thermogravimetric curves show the three stages of thermal transition owing to weight loss. The first significant weight loss is observed in the temperature range between 30 and 100  $^{\circ}$ C.

In this region, the weight loss increases with PSS wt% due to the residual water evaporation. The above result indicates that higher wt% of PSS increases the



hygroscopic nature of the PAT particles. The weight loss started at above 225 °C corresponds to gradual detachment of SO<sub>3</sub>H dopant from PAT particles and the loss of the sulfonic acid group by desulfonation. Almost the second weight loss ends at around 325 °C for lower wt% of PSS. The detachment of dopant is extended to 450 °C for higher weight ratios of PSS. The third weight loss corresponds to the decomposition of the main chain of PAT particles. The decomposition is started at around 325 and 450 °C for lower wt% and higher weight ratio of PSS, respectively.

## Conclusion

The PAT:PSS nanocolloidal particles were synthesized through the dispersion polymerization technique. The particle size and TEM analysis confirmed that the higher wt% of PSS reduces the particle size to nano-range around 100 nm from 2 μm. The functional group and doping level of the PAT particles with respect to different wt% of PSS are confirmed through the studies of FT-IR and elemental analysis. The reduction in conjugation length of PAT particles is interpreted in SEM and UV–visible studies. The higher wt% of PSS increased the thermal stability of PAT:PSS nanoparticles.

**Acknowledgments** The authors are thankful to sophisticated test and instrumentation center, Cochin (Kerala), and Birla Institute of Technology, Mesra, Ranchi for providing instrumental facilities.

**Open Access** This article is distributed under the terms of the Creative Commons Attribution License which permits any use, distribution, and reproduction in any medium, provided the original author(s) and the source are credited.

## References

- Olmedo, L., Hourquebie, P., Jousse, F.: Handbook of organic conductive molecules and polymers. In: Nalwa, H.S., (ed.) John Wiley and Sons Ltd, New York (1997)
- Yu, Y., Mao, H., Chen, L., Lu, X., Zhang, W., Wei, Y.: Synthesis of a novel oligoaniline: “Dumbbell-shaped” oligoaniline. *Macromol. Rapid Commun.* **25**, 664–668 (2004)
- Chao, D., Chen, J., Lu, X., Chen, L., Zhang, W., Wei, Y.: SEM study of the morphology of high molecular weight polyaniline. *Synth. Met.* **150**, 47–51 (2005)
- De Risi, F.R., D’Ilario, L., Martinelli, A.: Synthesis and characterization of epoxidized polybutadiene/polyaniline graft conducting copolymer. *Polym. Sci. A Polym. Chem.* **42**, 3082–3090 (2004)
- Lu, X., Yu, Y., Chen, L., Mao, H., Zhang, W., Wei, Y.: Preparation and characterization of polyaniline microwires containing CdS nanoparticles. *Chem. Commun.* **13**, 1522–1523 (2004)
- Kaneko, M., Nakamura, H.: Photo response of a liquid junction polyaniline films. *J. Chem. Soc. Chem. Commun.* **6**, 346–347 (1985)
- Paul, E.W., Ricco, A.J., Wrighton, M.S.: Resistance of polyaniline films as a function of electrochemical potential and the fabrication of polyaniline based microelectronic devices. *J. Phys. Chem.* **89**, 1441–1447 (1985)
- Chen, S.A., Fang, Y.: Polyaniline schottky barrier effect of doping on rectification and photovoltaic characteristics. *Synth. Met.* **60**, 215–222 (1993)
- Kitani, A., Yano, J., Sasaki, K.: ECD materials for the three primary colors developed by polyanilines. *J. Electroanal. Chem.* **209**, 227–232 (1986)
- Epstein, A.J., Yue, J.: Polyaniline compositions, process for their preparation and uses thereof. US Patent, No. 5237991 (1991)
- Svetlicic, V., Schmidt, A.J., Miller, L.L.: Conductometric sensors based on the hypersensitive response of plasticized polyaniline films to organic vapors. *Chem. Mater.* **10**, 3305–3307 (1998)
- Sukeerthi, S., Contractor, A.Q.: Molecular sensors and sensor arrays based on polyaniline microtubules. *Anal. Chem.* **68**, 779–783 (1996)
- Chunhua, L., Hui, P., Lijuan, Z., Guo-Liang, L., Yiting, W., Jadranka, T.S.: Formation of nano-microstructures of polyaniline and its derivatives. *Macromolecules* **44**, 6899–6907 (2011)
- Savitha, P., Sathyanarayana, D.N.: Copolymers of aniline with o-toluidine and m-toluidine: synthesis and characterization. *Polym. Int.* **53**, 106–112 (2004)
- Lim, V.W.L., Kang, E.T., Neoh, K.G., Ma, Z.H., Tan, K.L.: Determination of pyrrole- aniline copolymer composition by X-ray photoelectron microscopy. *Appl. Surf. Sci.* **181**, 317–326 (2001)
- Bae, W.J., Jo, W.H., Park, Y.H.: Preparation of polystyrene/polyaniline blends by in situ polymerization technique and their morphology and electrical property. *Synth. Met.* **132**, 239–244 (2003)
- Li, G., Martinez, C., Semancik, S.: Controlled electrophoretic patterning of polyaniline from a colloidal suspension. *J. Am. Chem. Soc.* **127**, 4903–4909 (2005)
- Chiou, N.R., Epstein, A.J.: Polyaniline nanofibers prepared by dilute polymerization. *Adv. Mater.* **17**, 1679–1683 (2005)
- Chen, S.A., Lee, H.S.: Structure and properties of poly(acrylic acid)-doped polyaniline. *Macromolecules* **28**, 2858–2866 (1995)
- Stejskal, J., Sulimenko, T., Prokes, J., Sapurina, I.: Polyaniline dispersions: coloured microparticles of variable density prepared using stabilizer mixtures. *Colloid Polym. Sci.* **278**, 654–658 (2000)
- Lee, K., Cho, S., Park, S.H., Heeger, A.J., Lee, C.W., Lee, S.H.: Metallic transport in polyaniline. *Nature* **441**, 65–68 (2006)
- Park, M.K., Onishi, K., Locklin, J., Caruso, F., Advincula, R.C.: Self-assembly and characterization of polyaniline and sulfonated polystyrene multilayer-coated colloidal particles and hollow shells. *Langmuir* **19**, 8550–8554 (2003)
- Ngamna, O., Morrin, A., Killard, A.J., Moulton, S.E., Symth, M.R., Wallace, G.G.: Inkjet printable polyaniline nanoformulations. *Langmuir* **23**, 8569–8574 (2007)
- Li, X., Dai, N., Wang, G., Song, X.: Water-dispersible conducting polyaniline/nano-SiO<sub>2</sub> composites without any stabilizer. *J. Appl. Polym. Sci.* **107**, 403–408 (2008)
- Huang, L.M., Tang, W.R., Wen, T.C.: Spatially electrodeposited platinum in polyaniline doped with poly(styrene sulfonic acid) for methanol oxidation. *J. Power Sour.* **164**, 519–526 (2007)
- Reneker, D.H., Chum, I.: Nanometre diameter fibres of polymer, produced by electrospinning. *Nanotechnology* **7**, 216–223 (1996)
- Liu, F.J., Huang, L.M., Wen, T.C., Gopalan, A., Hung, J.S.: Interfacial synthesis of platinum loaded polyaniline nanowires in poly(styrene sulfonic acid). *Mater. Lett.* **61**, 4400–4405 (2007)
- Bezduzhna, E., Ritter, H.: Microwave accelerated synthesis of n-phenylmaleimide in a singlestep and polymerization in bulk. *Macromol. Rapid Commun.* **26**, 1087–1092 (2005)



29. Dhawan, S.K., Trivedi, D.C.: Influence of polymerization conditions on the properties of poly(2-methylaniline) and its copolymer with aniline. *Synth. Met.* **60**, 63–66 (1993)
30. Huang, M.R., Li, X.G., Yang, Y.L., Wang, X.S., Yan, D.: Oxidative copolymers of aniline with o-toluidine: Their structure and thermal properties. *J. Appl. Polym. Sci.* **81**, 1838–1847 (2001)
31. Huang, J., Kaner, R.B.: The intrinsic nanofibrillar morphology of polyaniline. *Chem. Commun.* **4**, 367–376 (2006)
32. Stejskal, J., Sapurina, I., Trchova, M.: Polyaniline nanostructures and the role of aniline oligomers in their formation. *Prog. Polym. Sci.* **35**, 1420–1481 (2010)
33. Dispenza, C., Sabatino, M.A., Chmielewska, D., LoPresti., Battaglia, G.: Inherently fluorescent polyaniline nanoparticles in a dynamic landscape. *React. Funct. Polym.* **72**, 185–197 (2012)

